

Are back-to-back particle–antiparticle correlations observable in high energy nuclear collisions?

Jörn Knoll^{1,*}

¹*GSI Helmholtzzentrum für Schwerionenforschung GmbH, Planckstr. 1, 64291 Darmstadt, Germany*

(Dated: October 22, 2010)

Analytical formulae are presented which provide quantitative estimates for the suppression of the anticipated back-to-back particle–antiparticle correlations in high energy nuclear collisions due to the finite duration of the transition dynamics. They show that it is unlikely to observe the effect.

PACS numbers: 14.40.-n

Keywords: particle–antiparticle correlations, heavy-ion collisions

I. INTRODUCTION

In 1996 Asakawa and Csörgö [1] suggested that back-to-back particle–antiparticle correlations should be observable in high-energy nuclear collisions, see also earlier considerations in Refs. [2, 3]. Based on a sudden transition assumption huge effects were predicted for this phenomenon. About a further dozen applications followed. In a subsequent paper together with Gyulassy [4] it was shown that the finite duration τ of the transition reduces the effect. In that paper, however, the authors used a discontinuous and therefore unrealistic transition profile that led to large ultraviolet Fourier components and thus to a very moderate reduction of the effect of order $1/((2\omega\tau)^2 + 1)$. Here 2ω is the energy required to produce the pair. In this short note it will be shown that with a smooth transition profile the suppression is rather

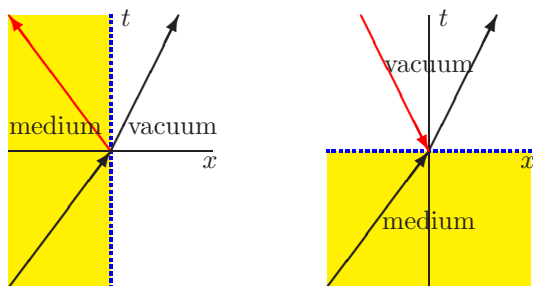


FIG. 1: Optical ray pictures in space-time. Left: the standard reflection-transmission situation, where a wave traverses from one medium (yellow) to another one (e.g. vacuum) at a spatial interface. Right: the sudden transition in time from the medium to the vacuum; here the frequency ω is discontinuous, creating a second component with negative ω which has the interpretation of an antiparticle with opposite momentum. The (blue) dashed line separates the media, the arrow sense distinguishes between particle and antiparticle. By means of Lorentz transformations the concept can directly be generalized to hyper-planes and even to curved hyper-surfaces.

exponential, $\sim e^{-4\omega\tau}$, deferring to observe the effect for realistic transition durations.

II. THE SUDDEN PICTURE

The main assumption of the original approach [1] is the sudden change from the in-medium situation to that in vacuum. The authors used the Bogolioubov-Valatin (BV) transformation to describe the effect, a picture that may not be so intuitive for many of us. Indeed the effect is nothing else than a standard “reflection–transmission” problem at the interface of two media, a well known problem in physics, in particular in optics. Thus, transcribing our wisdom from the spatial situation, like a wave traversing from one medium to another one at a sharp interface (see Fig. 1 left) to the here considered sudden transition in time (Fig. 1 right), precisely recovers the results presented in [1, 4]. The common boundary condition is that one has one incoming wave and two time-forward propagating outgoing wave components. As in Refs. [1, 4] we restrict the discussion to (charged) relativistic bosons described by the Klein-Gordon (KG) equation. For the sudden case the wave functions with positive and negative energies prior and post to the sudden transition can then be written as (using units with $\hbar=c=1$)

$$\Psi_{\text{med}}^{\pm}(x) = \frac{1}{\sqrt{2\Omega_{\mathbf{k}}}} e^{\mp i\Omega_{\mathbf{k}}t + i\mathbf{k}\mathbf{x}} \quad \text{for } t < 0, \quad (1)$$

$$\Psi_{\text{vac}}^{\pm}(x) = \frac{1}{\sqrt{2\omega_{\mathbf{k}}}} (c_{\mathbf{k}} e^{\mp i\omega_{\mathbf{k}}t + i\mathbf{k}\mathbf{x}} + s_{\mathbf{k}} e^{\pm i\omega_{\mathbf{k}}t + i\mathbf{k}\mathbf{x}}). \quad (2)$$

Here $\Omega_{\mathbf{k}}$ and $\omega_{\mathbf{k}}$ are the single-particle energies at momentum \mathbf{k} in the two media. Continuity of $\Psi(x)$ and of $\partial\Psi(i)/\partial t$ at transition time $t = 0$ determines the coefficients on the vacuum side to

$$c_{\mathbf{k}} = \frac{1}{2} \left(\sqrt{\frac{\omega_{\mathbf{k}}}{\Omega_{\mathbf{k}}}} + \sqrt{\frac{\Omega_{\mathbf{k}}}{\omega_{\mathbf{k}}}} \right) = \cosh[r_{\mathbf{k}}], \quad (3)$$

$$s_{\mathbf{k}} = \frac{1}{2} \left(\sqrt{\frac{\omega_{\mathbf{k}}}{\Omega_{\mathbf{k}}}} - \sqrt{\frac{\Omega_{\mathbf{k}}}{\omega_{\mathbf{k}}}} \right) = \sinh[r_{\mathbf{k}}], \quad (4)$$

$$\text{with } r_{\mathbf{k}} = \frac{1}{2} \ln \frac{\omega_{\mathbf{k}}}{\Omega_{\mathbf{k}}}, \quad (5)$$

while due to the spatial homogeneity the spatial momentum \mathbf{k} remains unchanged. Within the standard rela-

*e-mail: j.knoll@gsi.de

tivistic quantum field theory (RQFT) interpretation of the negative energy components as antiparticles with opposite spatial momenta, cf. Fig. 1 right frame, this result identically reproduces that given in Refs. [1, 4] within the BV picture. In particular the ratio of the antiparticle over particle component on the vacuum side

$$\mathcal{A} = \left| \frac{s_{\mathbf{k}}}{c_{\mathbf{k}}} \right| = \left| \frac{\Omega_{\mathbf{k}} - \omega_{\mathbf{k}}}{\Omega_{\mathbf{k}} + \omega_{\mathbf{k}}} \right| \quad (6)$$

is the analog of the well known reflection coefficient for a wave traversing from one medium to another (Fig. 1 left)

$$\mathcal{R} = \left| \frac{K - k}{K + k} \right|, \quad (7)$$

where K and k denote the moduli of the spatial momenta in the two media. In the spatial case solely k_{\perp} is discontinuous (ω and \mathbf{k}_{\parallel} are continuous). In the sudden case, however, \mathbf{k} is continuous, while the discontinuity in time causes a discontinuity in ω thereby creating a second component with negative ω , i.e. an antiparticle with opposite spatial momentum \mathbf{k} (Fig. 1 right frame). This mechanism led to the back-to-back particle–antiparticle correlation picture advocated in Ref. [1]. Besides small antiparticle components arising from the existing particles in the medium, the time dependent interaction can also create genuine particle–antiparticle pairs out of the vacuum. The latter, which is the bosonic analog to the Dirac case, where a time-dependent interaction pulse can lift a particle from the filled Dirac sea to the particle space¹, can formally be included by adding a “+1” to the boson occupations $n_{\mathbf{k}}$ of the antiparticles. After the transition the one-body density becomes

$$n_1(\mathbf{k}) = |c_{\mathbf{k}}|^2 n_{\mathbf{k}} + |s_{\mathbf{k}}|^2 (n_{\mathbf{k}} + 1) \quad (8)$$

$$n_{\mathbf{k}} = \frac{1}{\exp(|\Omega_{\mathbf{k}}|/T) + 1}, \quad (9)$$

while the back-to-back correlation function of particle–antiparticle pairs over the product of single yields becomes [4]

$$C_2(\mathbf{k}, -\mathbf{k}) = \frac{n_2(\mathbf{k}, -\mathbf{k})}{n_1(\mathbf{k})n_1(-\mathbf{k})} \quad (10)$$

$$= 1 + \frac{|c_{\mathbf{k}}^* s_{\mathbf{k}} n_{\mathbf{k}} + c_{-\mathbf{k}}^* s_{-\mathbf{k}} (n_{-\mathbf{k}} + 1)|^2}{n_1(\mathbf{k})n_1(-\mathbf{k})} \quad (11)$$

$$\xrightarrow{|s_{\mathbf{k}}| \ll 1} 1 + |s_{\mathbf{k}}|^2 \left| \frac{2n_{\mathbf{k}} + 1}{n_{\mathbf{k}} + |s_{\mathbf{k}}|^2 (n_{\mathbf{k}} + 1)} \right|^2. \quad (12)$$

Due to the sudden pair creation processes this back-to-back correlation ratio can attain huge values, once the

statistical occupations $n_{\mathbf{k}}$ fall below $|s_{\mathbf{k}}|^2$. The subsequent considerations will show that this effect is an artifact resulting from the sudden limit.

III. THE CONTINUOUS TRANSITION CASE

Compared to the BV transformation considered in [1, 4] the wave dynamical picture used here can easily be generalized to the continuous transition case by solving the time dependent Klein-Gordon equation (suppressing in the following the dependence on spatial momentum \mathbf{k})

$$\partial_t^2 \Psi(t) + \Omega^2(t) \Psi(t) = 0 \quad (13)$$

for a smoothly time-dependent dispersion relation

$$\Omega^2(t) = \omega^2 + \Pi^{\text{R}}(t) = \omega^2 + \Pi^{\text{R}}(-\infty)F(t). \quad (14)$$

Here negative times refer to the situation in the medium where Π^{R} denotes the time-dependent retarded polarization function², while the vacuum case is attained for large positive times. Thereby $F(t)$, cf. Fig. 2 below, will later be used to parameterize the transition profile.

Besides direct numerical solutions of (13), there are approximate analytical methods to obtain the reflection coefficient. These concern the single reflection limit as well as refined semi-classical methods.

A. Single reflection approximation

A simple generalisation of the sudden limit towards a continuous treatment is provided by the single reflection approximation (SR). In this scheme the continuous function $F(t)$ is approximated by a sequence of steps each providing a reflected wave component according to (6). In the continuum limit the coherent sum of these partial reflections leads to

$$\mathcal{A}^{\text{SR}} = \int_{-\infty}^{\infty} dt \frac{\dot{\Omega}(t)}{2\Omega(t)} \exp\left(-2i \int_0^t dt' \Omega(t')\right) \quad (15)$$

$$\approx \int_{-\infty}^{\infty} dt \Psi_f^*(t) \dot{\Omega}(t) \Psi_i(t). \quad (16)$$

Thereby the appropriate phase coherence is approximately provided by describing the unreflected wave components of particles (i) and their antiparticle partners (f) in the semi-classical (WKB) limit as

$$\Psi_i(t) = \Psi_f^*(t) \approx \exp(-i \int_0^t dt' \Omega(t')) / \sqrt{2\Omega(t)}. \quad (17)$$

¹ In the Dirac case also spatial transitions (Fig. 1 left) lead to spontaneous pair production, known as Klein paradox [5], once the vector potential changes by more than twice the rest mass.

² In general the polarization function Π can also be non-local in time and thus be energy dependent in the semi-classical interpretation. Then the mapping from the medium to the vacuum case will involve corresponding “ z ”-factors, $z = 1/(1 - \partial \text{Re} \Pi^{\text{R}} / \partial \omega^2)$, as e.g. shown in Kadanoff-Baym final-state interaction picture [6]. For the example cases discussed here we will discard such generalization and stick to time local cases.

Since $\dot{\Omega}$ is peaked and limited to a narrow range in t , the antiparticle amplitude \mathcal{A} is essentially given by the time Fourier transformed of $\dot{\Omega}(t)$, i.e.

$$|s_{\mathbf{k}}| \approx |\mathcal{A}^{\text{SR}}| \approx \left| \frac{\Omega - \omega}{\Omega + \omega} \right| |g(2\bar{\omega})| \quad \text{with} \quad (18)$$

$$g(\omega) = \int dt e^{-i\omega t} f(t), \quad f(t) = -\frac{dF(t)}{dt}. \quad (19)$$

with abbreviations $\Omega = \Omega(-\infty)$ and $\omega = \Omega(+\infty)$. Thereby $\bar{\omega} = \Omega(\bar{t})$ is chosen around the maximum of $\dot{\Omega}$. As multiple reflections at the different steps are suppressed, the approximation solely recovers terms linear in $\Delta\Omega = \Omega - \omega$. Compared to the sudden result (6) the suppression of the antiparticle amplitude caused by the finite duration of the transition is then given by $g(2\bar{\omega})$. This was also the approximation scheme used in Ref. [4] where, however, a completely unrealistic form for $f(t)$ was considered, namely $f(t) = \Theta(t) \exp[-t/\tau]/\tau$. This form contains a sharp jump which leads to unrealistically high Fourier components for large ω , and thus only to a very moderate suppression of the effect! More realistic forms for $\Omega(t)$ generally will lead to exponential suppression factors, as e.g. for the following analytically solvable cases

	$F(t)$	$f(t)$	$g(\omega)$
(a)	$\frac{1}{2} - \frac{1}{\pi} \arctan \frac{\pi t}{2\tau}$	$\frac{2\tau}{\pi^2 t^2 + 4\tau^2}$	$e^{- 2\omega\tau/\pi }$
(b)	$\frac{1}{2} - \frac{1}{\pi} \arctan(\sinh \frac{\pi t}{2\tau})$	$\frac{1}{2\tau \cosh(\pi t/(2\tau))}$	$\frac{1}{\cosh(\omega\tau)}$
(c)	$\frac{1}{\exp(2t/\tau)+1}$	$\frac{1}{2\tau \cosh^2(t/\tau)}$	$\frac{\pi\omega\tau}{2 \sinh(\pi\omega\tau/2)}$

(20)

In order to assure comparable results all functions are chosen such that $F(t)$ monotonically falls from 1 to 0 with a maximum time derivative at $t = 0$ of $f(0) = -\dot{F}(0) = 1/(2\tau)$, cf. Fig. 2. Then τ is approximately the “half time” for the change in $\Omega^2(t)$. For short transitions times $\tau \rightarrow 0$, one verifies the sudden result (6) since then $g(2\omega) \rightarrow 1$. For large $\bar{\omega}\tau$ all three cases indeed lead to exponential suppression factors

$$|g(2\bar{\omega})|^2 \xrightarrow{\bar{\omega}\tau \gg 1} C e^{-4\alpha\bar{\omega}\tau} \quad (21)$$

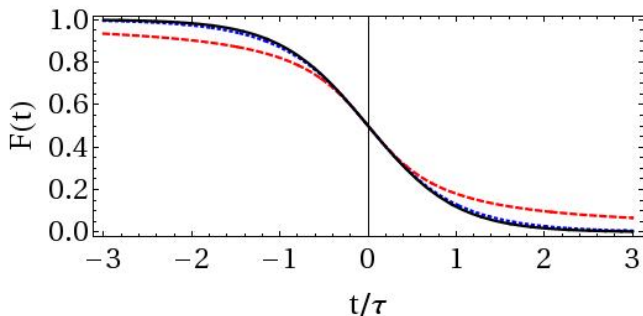


FIG. 2: (Color online) $F(t)$ for the three example cases of table (20), (a) red dashed, (b) blue dotted, (c) black full line.

with $C = (1, 4, (4\pi\bar{\omega}\tau)^2)$ and $\alpha = (2/\pi, 1, \pi/2)$ for the cases (a) to (c) of (20). Thereby the asymptotic exponential behavior is directly determined by the imaginary part of the nearest complex pole position of $F(t)$.

The physical case where the polarization function is switched on and off, i.e. where $F(t)$ takes the form of a bell shape can simply be retrieved by replacing $F(t)$ by its time derivative $F_{\text{bell}}(t) = 2\tau f(t)$ with $f(t)$ from table (20). The corresponding “pulse” has a maximum of 1 and a time integral of 2τ . The suppression factor (21) for the pair production then will simply attain an additional pre-exponential factor of $(4\bar{\omega}\tau)^2$.

B. Complex semi-classical method (CWKB)

An alternative method to access the reflected wave component is provided by the *complex* WKB method [7]. In that case the “reflected” wave component results from the analytic continuation of the “unreflected” WKB wave Ψ_1 , cf. Eq. (17), around the nearest *complex valued* turning point t_0 where $\Omega^2(t_0) = 0$. Then the reflection coefficients \mathcal{R} or \mathcal{A} are given by [7]

$$\mathcal{A}^{\text{CWKB}} = \exp[-2|\text{Im } S(t_0, t)|] \quad (\text{for real } t), \quad (22)$$

where

$$S(t_0, t) = \int_{t_0}^t dt' \sqrt{\Omega^2(t')}, \quad (23)$$

is the action integral from the nearest complex turning point t_0 to some time t on the real axis. Since the action integral along the real axis does not contribute to $\text{Im } S$, a rough estimate can simply be obtained by choosing the integration contour starting from t_0 just parallel to the imaginary axis till the real axis. Assuming that along this contour the integrand can essentially be approximated by its value on the real axis one obtains the estimate

$$\text{Im } S(t_0) \approx \Omega(\text{Re } t_0) \text{Im } t_0. \quad (24)$$

For the three analytic cases of table (20) one verifies that the complex turning points are located close to the pole positions of $F(t)$ with values for $\text{Im } t_0 = \alpha\tau$ with $\alpha = 2/\pi, 1$ and $\pi/2$, respectively for the cases (a) to (c) in (20). Thus the pair creation rate then becomes

$$|s_{\mathbf{k}}|^2 \approx |\mathcal{A}^{\text{CWKB}}|^2 \approx e^{-4\alpha\bar{\omega}\tau} \quad (25)$$

in agreement with the leading exponential terms of the single reflection approximation given in (21).

C. The exact Fermi function case

The Fermi-function case (20c) is particularly interesting, since the corresponding KG equation (13) can be solved in closed form, providing the exact result [8]

$$\mathcal{A}_{\text{Fermi}}^2 = \left| \frac{\sinh(\pi(\Omega - \omega)\tau/2)}{\sinh(\pi(\Omega + \omega)\tau/2)} \right|^2. \quad (26)$$

It generalizes the sudden result (6) to the continuous Fermi-function case (20c) and further confirms the limiting cases of the single-reflection approximation (18) and the CWKB result (25) within their validity ranges. Also the corresponding action integral (23) and thus its imaginary part can be obtained in closed form

$$S_{\text{Fermi}}(t_0, t) = \Omega\tau \operatorname{artanh} \frac{\Omega(t)}{\Omega} - \omega\tau \operatorname{artanh} \frac{\Omega(t)}{\omega} \quad (27)$$

$$|\operatorname{Im} S_{\text{Fermi}}(t_0, t)| = \frac{\pi}{2} \operatorname{Min}(\Omega, \omega) \tau \quad (\text{for real } t), \quad (28)$$

the imaginary part resulting from that artanh function with argument larger than 1. The corresponding CWKB amplitude (22) then becomes

$$|\mathcal{A}_{\text{Fermi}}^{\text{CWKB}}|^2 = \exp[-2\pi \operatorname{Min}(\Omega, \omega) \tau], \quad (29)$$

in full compliance with the semi-classical limit ($\omega\tau \gg 1$, $\Delta\Omega\tau \gg 1$) of the exact Fermi-function result (26).

IV. SUMMARY AND CONCLUDING REMARKS

For nuclear collisions with a freeze-out temperature T and a correspondingly smooth time dependence of the polarization function Π , the back-to-back correlation (12) can then be estimated to

$$|c_2(\mathbf{k}, -\mathbf{k}) - 1| \approx \mathcal{O}(|s_{\mathbf{k}}|^2/n_{\mathbf{k}}^2) \approx e^{-\Omega_{\mathbf{k}}(4a\tau - 2/T)}, \quad (30)$$

valid for $|s_{\mathbf{k}}|^2 \ll n_{\mathbf{k}} \ll 1$. Thus, the original effect advocated in Refs. [1, 4] of unlimitedly large correlations with increasing $\Omega_{\mathbf{k}}$ resulting in the sudden case ($\tau = 0$) turns into the opposite behavior, once the duration time τ exceeds the inverse temperature $1/T$. Already for charged pion pairs ($\pi^+\pi^-$) with $\Omega_{\mathbf{k}} \approx 300$ MeV the correlation (30) falls below the 10^{-5} level for transition times τ beyond 3 fm/c, at typical freeze-out temperatures of $T \approx 140$ MeV. Since optical potentials are generally proportional to the density, the characteristic transition-time scale is rather given by the expansion-time scale [9–11] in nuclear collisions. Its full-width-half-maximum values generally lie beyond 4 fm/c, leading to

even larger suppression factors. Thus, the pair creation process due to the time variation of the mean field becomes unmeasurably small in nuclear collisions.

The discussed particle–antiparticle correlation effect rests on a coherent single-particle picture. Among others it largely ignores collisional effects that are known to dominate the nuclear collision dynamics. Thus, in individual events the one-body field will depart from the ensemble mean due to fluctuations caused by stochastic processes. Such microscopic processes can involve much shorter time scales which, however, are also ultra violet restricted by the frequencies accessible in the system. For thermal systems this limit is given by the inverse temperature scale, i.e. $\tau > 1/T$, limiting the “thermal” production of *hard* probes, such as the particle–antiparticle pairs. Such stochastic processes generally add incoherently to the two-particle yield. Therefore they can appropriately be included in transport codes by simulating the corresponding microscopic collision processes. The resulting pair correlations, however, are no longer strictly back-to-back, as they are influenced by thermal motion.

The question, whether a process can be treated in the sudden limit or not, depends on its intrinsic quantum time scale resulting from the uncertainty principle to $\tau_Q \approx 1/\Delta E$, where ΔE is the energy transfer. Driven by a certain field, the dynamics is “sudden”, if the typical time duration τ , during which the field changes, is short compared to τ_Q : then the wave functions stay “inert” across the transition thereby creating several components in the eigenstates of the “new” Hamiltonian. In the opposite limit $\tau \gg \tau_Q$ the quantum states change and adjust adiabatically. As shown here for the pair creation case, where $\Delta E = 2\Omega_{\mathbf{k}}$, the creation of states involving an energy transfer $\Delta E \gg 1/\tau$ then becomes exponentially suppressed.

Acknowledgement

The author acknowledges constructive discussions with P. Braun-Munzinger, B. Friman and D.N. Voskresensky.

-
- [1] M. Asakawa and T. Csörgő, *Heavy Ion Phys.* **4**, 233 (1996), hep-ph/9612331.
 - [2] A. Vourdas and R. M. Weiner, *Phys. Rev.* **D38**, 2209 (1988).
 - [3] L. V. Razumov and R. M. Weiner, *Phys. Lett.* **B348**, 133 (1995), hep-ph/9411244.
 - [4] M. Asakawa, T. Csörgő, and M. Gyulassy, *Phys. Rev. Lett.* **83**, 4013 (1999), nucl-th/9810034.
 - [5] O. Klein, *Z. Phys.* **53**, 157 (1929).
 - [6] J. Knoll (2010), to be published.
 - [7] J. Knoll and R. Schaeffer, *Annals Phys.* **97**, 307 (1976).
 - [8] S. Flügge, *Rechenmethoden der Quantentheorie* (Springer Berlin Heidelberg New York, 1965), exercise 22.
 - [9] J. Knoll, *Nucl. Phys.* **A821**, 235 (2009), 0803.2343.
 - [10] J. Knoll, *Acta Phys. Polon.* **B40**, 1037 (2009), 0902.2373.
 - [11] B. Friman et al., *The CBM Physics Book, Compressed Baryonic Matter in Laboratory Experiments; Lecture Notes in Physics*, Vol. 814 (Springer Berlin Heidelberg New York, 2010), Part III, Sect. 5.8.